Fe(II) Induced Reduction of Incorporated U(VI) to U(V) in Goethite

Olwen Stagg, Katherine Morris, Andy Lam, Alexandra Navrotsky, Jesús M. Velázquez, Bianca Schacherl, Tonya Vitova, Jörg Rothe, Jurij Galanzew, Anke Neumann, Paul Lythgoe, Liam Abrahamsen-Mills, and Samuel Shaw*

ABSTRACT: Over 60 years of nuclear activities have resulted in a global legacy of radioactive wastes, with uranium considered a key radionuclide in both disposal and contaminated land scenarios. With the understanding that U has been incorporated into a range of iron (oxyhydr)oxides, these minerals may be considered a secondary barrier to the migration of radionuclides in the environment. However, the long term stability of U incorporated iron (oxyhydr)oxides is largely unknown, with the end fate of incorporated species potentially impacted by biogeochemical processes. In particular, studies show that significant electron transfer may occur between stable iron (oxyhydr)oxides such as goethite and adsorbed Fe(II). These interactions can also induce varying degrees of iron (oxyhydr)oxide recrystallization (<4% to >90%). Here, the fate of U(VI) incorporated goethite during exposure to Fe(II) was investigated using geochemical analysis and X ray absorption spectroscopy (XAS). Analysis of XAS spectra revealed that incorporated U(VI) was reduced to U(V) as the reaction with Fe(II) progressed, with minimal recrystallization (approximately 2%) of the goethite phase. These results therefore indicate that U may remain incorporated within goethite as U(V) even under iron reducing conditions. This develops the concept of iron (oxyhydr)oxides acting as a secondary barrier to radionuclide migration in the environment.

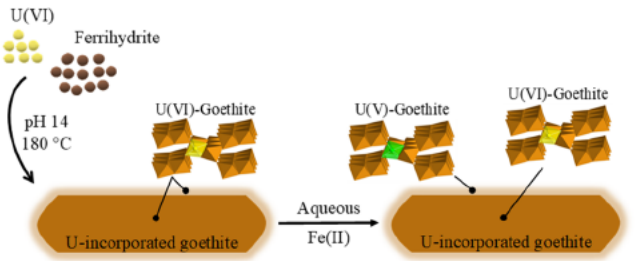

KEYWORDS: *Fe(II), U(VI,V), iron (oxyhydr)oxides, XAS, HR XANES*

INTRODUCTION

Uranium (U) is a widespread environmental contaminant and a key radionuclide in many radioactive wastes.[1,2] As these wastes can take extensive time (over tens of thousands of years) to decay to safe levels, a deep underground geological disposal facility (GDF) is widely accepted as the most favorable disposal route.[2] Within a typical GDF, steel and engineering structures such as rock bolts will corrode over time, forming iron (oxyhydr)oxide minerals in and around the repository. Given that iron (oxyhydr)oxides are also abundant in the wastes and in the geosphere, understanding their interactions with U will provide further understanding of the long term fate of U species.[2,3] To this end, the ability of U to incorporate into the crystal structure of iron (oxyhydr)oxides has been well established in recent years, with the inference that long term immobilization of U species through incorporation may occur.[4−16] However, although iron (oxyhydr)oxides have the potential to act as a secondary barrier to uranium migration, the long term fate and stability of incorporated U in the environment is largely unknown.

In subsurface environmental and geological systems, U mainly exists as either U(VI) or U(IV), with the highly mobile uranyl ion ($U(VI)O_2^{2+}$) forming under oxic conditions and immobile U(IV) phases (e.g., UO_2 and noncrystalline U(IV)) dominating in anoxic environments.[1,17,18] Although U(V) species may also form, they have typically been considered transient in the environment, with studies reporting rapid U(V) disproportionation to U(IV) and U(VI).[19] However, recent work has demonstrated that U(V) can be stabilized as an incorporated species on reaction with iron (oxyhydr)oxides, suggesting it may be more environmentally relevant than previously thought.[6−8,16]

Interactions with iron (oxyhydr)oxide phases play an important role in the environmental mobility of U, with U retardation occurring both by adsorption to mineral surfaces and by incorporation into a variety of iron (oxyhydr)oxide phases (i.e., goethite, hematite, magnetite, and green rust).[17,20−23] In the environment, the formation of crystalline iron (oxyhydr)oxide phases, such as goethite (α FeOOH), often occurs by the transformation of poorly ordered ferrihydrite. As ferrihydrite dissolution is a key step in this

mineral transformation pathway, the reaction may proceed by either the long term aging of ferrihydrite, or by Fe(II) catalyzed reductive dissolution.[24,25] The potential for U(V) to become incorporated during this Fe(II) catalyzed trans formation has been demonstrated, albeit often with mixed phases of iron (oxyhydr)oxides, residual starting material or mixed valence U in the final product.[6,12−16] The incorporation mechanism for U(V) into goethite has been proposed to occur via the sorption of U(VI) onto the ferrihydrite surface. The U(VI) forms a bidentate inner sphere complex, which is then reduced to U(V) by electron transfer from Fe(II) as the crystallization to goethite proceeds.[16] This reduction enables the elongation of the uranyl axial oxygen bonds to occur, resulting in the octahedral coordination of U(V) in a uranate like configuration (i.e., 6 U−O bonds at 2.18 Å).[16] The final step is then continued goethite growth, substituting U(V) for Fe(III) in an octahedral position within the goethite structure.[16] This coordination environment is similar to that reported for an incorporated uranate like U(V), formed on coprecipitation with magnetite and green rust.[7,8] Conversely, U(VI) was proposed to inhibit goethite growth by oriented attachment, as an incorporated uranyl moiety would break an edge sharing arrangement in the local structure and therefore be highly destabilizing.[26] Overall, this work concluded that incorporation of a U(VI) uranyl moiety was less favorable, in contrast to a uranate like U(V) which requires minimal distortion to the goethite structure.

Studies have indicated that incorporated U(V) species are resistant to oxidation, suggesting that incorporation of U into iron (oxyhydr)oxides may limit remobilization in the environ ment.[8,15] Although various studies have demonstrated the ability for iron (oxyhydr)oxides to incorporate U, questions still remain as to the long term fate. In particular, geochemical conditions in the environment will evolve over time, with iron reducing conditions leading to Fe(II) in the subsurface. Significant electron transfer has been shown to occur between adsorbed Fe(II) and structural Fe(III) in stable iron (oxyhydr)oxides, including goethite.[27−31] Additionally, in some studies electron transfer was proceeded by the physical exchange of structural Fe atoms with aqueous Fe.[32−35] The use of isotopic tracers has demonstrated that the extent of this Fe atom exchange is strongly dependent on pH, crystallinity, particle size, and contaminant substitution. Consequently, goethite may undergo either minimal recrystallization (<4%) or up to near complete (>90%) exchange of structural Fe(III) on exposure to Fe(II).[34−38] Moreover, electron transfer from adsorbed Fe(II) has resulted in incorporated contaminant species being either reduced (e.g., 44% reduction from Co(III) goethite to Co(II))[39] and/or released to solution (e.g., up to 28% released from Ni goethite).[39−41] Conse quently, electron transfer from adsorbed Fe(II) could affect the speciation of an incorporated redox active U contaminant, with the long term fate of U poorly understood.

Clearly, investigating the incorporation of U(VI) and U(V) into goethite, and assessing the impact of exposure to Fe(II), is important for understanding the long term fate of U in engineered and natural environments. In the current study, U(VI) incorporated goethite was synthesized and reacted with aqueous Fe(II); a pure U(V) goethite standard was also synthesized. The impact of electron transfer on U speciation was assessed by X ray absorption spectroscopy (XAS), using a combination of U M_{IV} edge and L_{III} edge spectroscopy. Additionally, a ^{57}Fe isotopic tracer technique[34] was used to monitor if electron transfer from adsorbed Fe(II) to U(VI) goethite was proceeded by a physical exchange of Fe atoms between the structural Fe(III) and aqueous Fe(II) phases.

MATERIALS AND METHODS

U(VI)-Incorporated Goethite. U(VI) incorporated goe thite was prepared via a hydrothermal synthesis method, informed by Schwertmann and Cornell.[42] Briefly, iron(III) nitrate nonahydrate was dissolved in a uranyl(VI) nitrate solution and titrated to pH 14. The resulting slurry (200 ppm U) was then heated in a hydrothermal vessel at 180 °C for 24 h. The solid was then extracted and washed repeatedly (approximately 7 times) with deionized water (DIW), followed by six washes with 4 mM HCl (pH < 2.5) to remove adsorbed U(VI) from the goethite product.[21,43] The solid was subsequently washed several times with DIW and dried overnight at 40 °C. The resultant mineral phase was then confirmed using X ray diffraction (XRD). The U distribution within goethite was characterized by progressive dissolution, using 0.4 M HCl to remove near surface U, followed by acid digestion in 6 M HCl.[44] To investigate the effect of U concentration on mineral formation, a mixed hematite/ goethite phase was also synthesized using the same technique, but with the initial U concentration increased from approximately 200 ppm to 635 ppm U. A U(V) incorporated goethite standard was also prepared, following a method adapted from Massey et al.[16] (Section S1 of the Supporting Information, SI).

Batch Experiments with Aqueous Fe(II). All the following experiments were undertaken inside a Coy Cabinet anaerobic chamber under an atmosphere of 95% N_2/5% H_2. Deionized water was boiled and sparged with N_2 for at least 1 h prior to introduction to the anaerobic cabinet. Synthesized U(VI) goethite particles were then reacted with aqueous Fe(II) using a sacrificial batch reactor approach.[45] Briefly, a 0.1 M Fe(II) stock solution was prepared by dissolving 0.127 g $FeCl_2$ in 10 mL deionized water, followed by the addition of 50 μL 0.4 M HCl to prevent oxidation. An aliquot of the Fe(II) stock solution was then added to a 3 (*N* morpholino) propanesulfonic acid sodium salt (MOPS Na) buffer solution (25 mM) to achieve a concentration of approximately 1 mM Fe(II), and the pH was adjusted to 7.6 ± 0.1 by the addition of 5 M NaOH and equilibrated for 30 min. The reaction was initiated by the addition of U(VI) goethite powder (2 g/L) followed by sonication (<2 min) to ensure complete mixing; a parallel Fe(II) free control was also prepared. The batch experiments were wrapped in foil to prevent photo oxidation and left to mix on an end overend rotator at room temperature.

At selected time points batch experiments were sacrificed, and solid samples were collected for acid digestion and XAS analysis. Aqueous samples were filtered (0.2 μm), with measurements of aqueous U performed by inductively coupled plasma mass spectrometry (ICP MS) and total aqueous Fe by either inductively coupled atomic emission spectrometry (ICP AES) or by the ferrozine assay.[46] Under neutral pH conditions, total aqueous Fe measurements were assumed as equivalent to aqueous Fe(II).[46,47] For acid digestion, samples were washed with 0.4 M HCl (10 mL, 15 min) to extract adsorbed Fe(II) and near surface U. Residual U incorporated goethite was then slowly dissolved in 6 M HCl (10 mL) with aliquots taken at defined time intervals and the supernatant collected for analysis (filtered to 0.2 μm).

For XAS, solid samples were filtered, mounted and stored anaerobically at −80 °C. Prepared samples were then transported frozen to either the Diamond Light Source, U.K., or the KIT synchrotron, Germany for analysis. XAS spectra of the L_{III} edge were obtained at the I20 scanning beamline (Diamond Light Source), with M_{IV} edge high energy resolution fluorescence detected X ray absorption near edge structure (HERFD XANES) spectra obtained at the ACT station of the CAT ACT beamline at KIT (further details in Section S2). Interestingly, recent evidence suggests that uncertainties might be present in M_{IV} edge analyses,[48,49] thus the U oxidation state quantification values presented here are assumed to have an error of ±5%.

^{57}Fe-Tracer Experiment. To monitor if electron transfer between adsorbed Fe(II) and U(VI) goethite was proceeded by an atom exchange of structural Fe(III) and aqueous Fe(II), the Fe(II) reaction was repeated using an aqueous phase enriched with ^{57}Fe(II). Briefly, a stock solution was prepared by dissolving ^{57}Fe (>95% ^{57}Fe, CK Isotopes, Ltd.) in HCl overnight, followed by filtration (<0.2 μm) and dilution with DIW to a final concentration of approximately 0.1 M ^{57}Fe(II). A 25 mM MOPS Na buffer solution was then spiked with 1 mM aqueous ^{57}Fe(II) and the pH adjusted to 7.6 ± 0.2 by the addition of 5 M NaOH. After at least 30 min equilibration, an aliquot was taken for initial Fe(II) measurements, and the reaction was initiated by either the addition of U(VI) incorporated goethite or U free goethite powder (2 g/L) with end overend mixing for 21 days. The reaction was performed in either duplicate (U goethite) or triplicate (goethite control), with aliquots removed for analysis at selected time points. Analysis was then conducted similar to Neumann et al.[50] using either an ICP MS (Agilent 7500CX) or an ICP QQQ (Agilent 8800). The isotopic fraction of ^{57}Fe was calculated from the ICP MS/QQQ counts per second (cps) of 54, 56, 57, and 58 Fe isotopes, using the following equation:[50]

$$f^{57}\mathrm{Fe} = \frac{57_{cps}}{54_{cps} + 56_{cps} + 57_{cps} + 58_{cps}}$$

The percentage of Fe atom exchange was then calculated from the ^{57}Fe fraction using the mass balance approach.[32,37,50,51]

RESULTS AND DISCUSSION

The synthesized U(VI) and U(V) goethite samples were first analyzed by XRD to confirm the crystalline phases present (Figure S1). The XRD patterns showed that pure goethite phases had been produced, with no evidence for hematite or lepidocrocite contamination. Here, the high temperature synthesis technique for U(VI) goethite produced a more crystalline phase, as evidenced by the narrower diffraction peaks of the hydrothermally produced U(VI) goethite relative to the U(V) goethite, which was synthesized at room temperature. Additionally, XRD patterns were collected on an Fe(II) reacted sample (30 day) and the 30 day no Fe(II) control, which show that goethite remained as the only crystalline iron (oxyhydr)oxide phase. The 30 day XRD pattern showed no visual difference in the peaks or peak widths compared to the synthesized U(VI) goethite standard which confirmed that no change to the mineralogy/crystallinity had occurred during reaction with Fe(II). Additionally, following the complete dissolution of samples in 6 M HCl, the U content of the synthetic U(VI) and U(V) goethite standards was determined to be approximately 0.21(2) wt % (0.08 mol %) and 0.83 wt % (0.31 mol %), respectively.

Fe(II) Reaction with U-Goethite. To investigate the impact of Fe(II) exposure on U(VI) goethite stability, aqueous Fe(II) was reacted with synthesized U(VI) goethite. Analysis of the aqueous phase revealed an initial drop in aqueous ^{57}Fe(II) concentration from approximately 1 mM to 0.6 mM by 6 h. Given a molar excess of approximately 60 Fe(II)/U(VI), a decrease in aqueous Fe(II) resulting from the coupled oxidation/reduction of Fe(II)/U(VI) would not be observable. Therefore, this decrease in aqueous Fe(II) is thought to be due to sorption of Fe(II) to goethite, consistent with past work.[34,35,38,45] After the initial sorption, the aqueous Fe(II) concentration stabilized and remained relatively constant over 212 days (Figure 1).

To monitor if electron transfer from adsorbed Fe(II) to U(VI) goethite was followed by a physical movement of Fe atoms from the solid phase into the solution, an aqueous phase

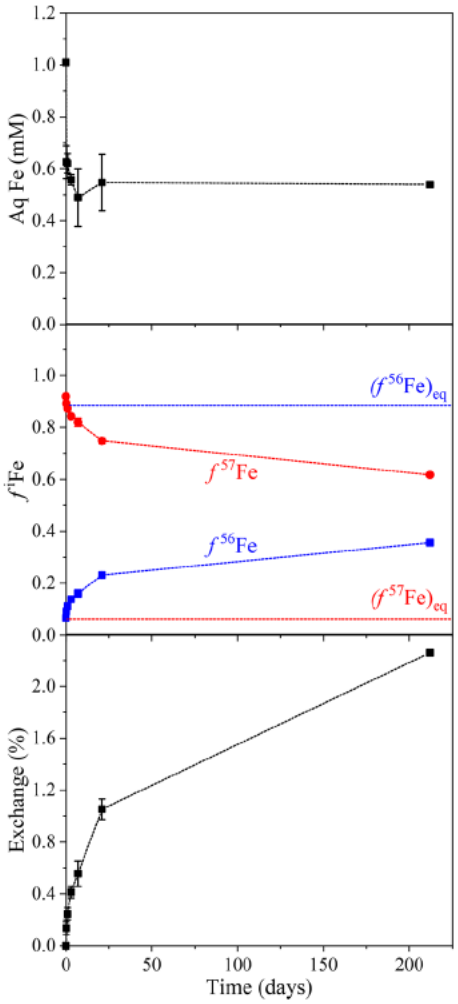

Figure 1. Aqueous data for the reaction of ^{57}Fe(II) with U(VI) goethite. Top panel shows the measurement of total Fe in the aqueous phase; the middle panel shows the isotopic fraction of ^{57}Fe and ^{56}Fe in the aqueous phase, with the dotted horizontal lines representing the values at complete mixing; and the bottom panel shows the percentage of Fe atom exchange calculated using the mass balance approach.[35] Data for 0.25−21 days are duplicates with error bars representing the range in values; the data point for 212 days is for a single reactor.

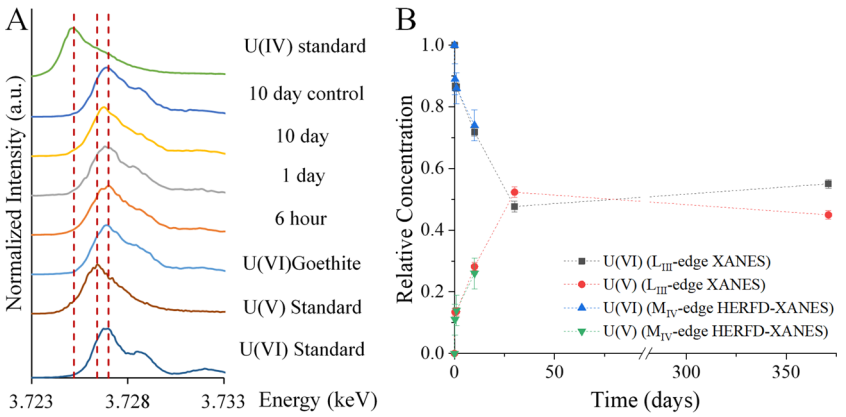

Figure 2. Panel (A) Uranium M_{IV} edge HERFD XANES, showing time points for Fe(II) reacted U(VI) goethite. Dotted red lines indicate peaks for standards $U(IV)O_2$, U(V) magnetite,[7] and U(VI) in sediment. Panel (B) Results from ITFA[56] of U M_{IV} edge HERFD XANES data and LCF of U L_{III} edge XANES data, showing the relative concentrations of U(V) and U(VI) in samples of Fe(II) reacted U(VI) goethite. Relative concentrations calculated from standards of U(VI) in sediment and U(V) in magnetite[7] for ITFA, and from synthesized U(VI) goethite and U(V) goethite standards for LCF.

^{57}Fe(II) tracer was used. This enabled the extent of recrystallization to be determined by measuring changes in the ^{57}Fe isotope fraction in the aqueous phase over time (Figure 1, middle panel).[35] During the reaction, there was a decrease in aqueous ^{57}Fe(II) and an ingress in aqueous ^{56}Fe(II), indicating that solid phase Fe(III) was exchanging with the ^{57}Fe(II) enriched aqueous phase. The extent of Fe atom exchange was then calculated from the Fe isotope ratio, which showed that after 21 days of reaction 1% of the solid phase had recrystallized, with just over 2% Fe atom exchange reached by 212 days (Figure 1). By comparison, studies have reported unsubstituted goethite to undergo various extents of Fe atom exchange under similar conditions of 0.5−1 mM Fe(II) and circumneutral pH, ranging from <4% to near complete (>90%) recrystallization.[35−38] Moreover, the extent of Fe atom exchange has been found to be dependent on a variety of factors such as crystallinity, surface area and pH.[32,35,38] In particular, research has shown that Fe atom exchange may decrease substantially in the presence of incorporated/sorbed contaminants, with Frierdich et al.[51] reporting a concurrent decrease in exchange (approximately 20−60% reduction) as Ni incorporation increased (0.5−2.5 mol %).[36,37,51,52] Given that the U concentration for incorporation in the current study is an order of magnitude lower (0.08 mol %) than the published studies, this seemed unlikely to be significantly hindering Fe atom exchange. This was further explored by preparing U free goethite powder, following the hydrothermal synthesis method described here. Reaction of this U free goethite control with ^{57}Fe(II) led to 0.8% exchange after 21 days, very similar to the 1% exchange (21 days) in the U(VI) goethite system. Previous work has highlighted that the extent of recrystallization is dependent on crystallinity, due to the annealing of defects being a key driving force for the process.[29,38] Furthermore, hydrothermally treating goethite has been shown to hinder electron transfer,[27] which has been suggested to be a key process leading to Fe atom exchange and Fe(II) catalyzed recrystallization of goethite.[34] Therefore, it is likely that the minimal exchange measured here (approximately 2%) is a reflection of a highly crystalline, hydrothermally synthesized product.

U Distribution. The initial preparation of the U(VI) goethite starting material involved an acid leach with 4 mM HCl to remove adsorbed uranium, prior to reaction with aqueous Fe(II). The U distribution in the 4 mM HCl acid leached U(VI) goethite starting material and Fe(II) reacted samples were then analyzed by progressive acid dissolution using 0.4 M HCl, to target the near surface U, followed by a slow acid digestion in 6 M HCl. For U(VI) goethite, the 0.4 M HCl showed an initial fast release of up to approximately 35% U with very little Fe dissolution (<0.9% Fe). This was followed by the congruent release of both U and Fe (linear relationship) during dissolution of the remaining U(VI) goethite in the 6 M HCl digestion (Figure S3). This indicates that in the U(VI) goethite starting material up to approximately 35% U is near surface incorporated, with the remaining U distributed throughout the bulk of goethite. By comparison, there was a constant linear relationship between U and Fe in the synthesized U(V) goethite reference material, with little 0.4 M HCl extractable U near surface incorporated (<10%), indicating an even distribution of U throughout the goethite structure (Figure S3).

Acid dissolution profiles of U(VI) goethite samples reacted with aqueous Fe(II) for 6 h, 1 day, 10 days, and 30 days (Figure S3) show that U distribution in goethite remained relatively constant. Aqueous analysis confirmed that U was not released to solution during the reaction with Fe(II), despite a significant proportion (approximately 40%) being near surface associated. Overall, this indicates that the hydrothermally synthesized U(VI) goethite is resistant to Fe(II) catalyzed recrystallization, reflective of the minimal levels (approximately 2%) of Fe atom exchange measured here, and therefore U remained bound within the solid phase.

Evolution of U Solid Phase Speciation. To determine U oxidation state, U M_{IV} edge HERFD XANES was used in combination with L_{III} edge XANES, similar to recent studies.[7,8,48,49,53−55] First, comparison to the peak position of standards (Figure 2A) confirmed that both the starting material and 10 day control goethite samples were predominantly U(VI), suggesting a pure U(VI) goethite phase. Analysis of the spectra also showed that there was no evidence for U(IV) in any of the samples. This confirmed that U likely remained incorporated within the goethite structure during reaction with aqueous Fe(II), as opposed to being released and reduced to a U(IV) surface precipitate by adsorbed Fe(II). Furthermore, ITFA[56] fitting of the HERFD

Table 1. Summary of EXAFS Fits in Comparison to Unsubstituted Goethite (Full Details in SI)

		goethite	U(VI)-goethite	6 h	24 h	10 day	30 day	30 day control	U(V)-goethite
U O_1	R (Å)		1.82	1.84	1.85	1.87		1.84	
	CN		0.8	0.8	0.8	0.8		1	
U O_2	R (Å)		2.03	2.06	2.06	2.08	1.98	2.07	
	CN		0.8	1	1	1	1	1	
U O_3	R (Å)		2.23	2.25	2.24	2.26	2.23	2.25	2.17
	CN		2.2	2.5	2.5	2.5	3	2	5.2
U O_4	R (Å)		2.42	2.44	2.44	2.45	2.43	2.42	2.45
	CN		2.2	1.7	1.7	1.7	2	2	1.8
U Fe_1	R (Å)	3.01	3.22	3.21	3.22	3.21	3.21	3.22	3.16
	CN	2	2	2	2	2	2	2	2
U Fe_2	R (Å)	3.29	3.44	3.44	3.45	3.44	3.45	3.45	3.32
	CN	2	2	2	2	2	2	2	2
U Fe_3	R (Å)	3.43	3.65	3.65	3.67	3.65	3.65	3.67	3.61
	CN	4	3	3	3	3	3	3	3
U Fe_4	R (Å)	4.58	4.71	4.71	4.73	4.71	4.67	4.77	4.70
	CN	2	1	1	1	1	1	1	2
U Fe_5	R (Å)	5.27 5.38	5.32	5.31	5.31	5.31	5.32	5.34	5.36
	CN	6	2	2	2	2	3	4	6
U Fe_6	R (Å)	5.47 5.66	5.63	5.62	5.60	5.63	5.62	5.58	5.61
	CN	10	2	2	2	2	4	4	8
U Fe_7	R (Å)	5.99	5.90	5.90	5.90	5.92	5.88		5.89
	CN	2	2	2	2	2	3		4

XANES spectra, in combination with the U(VI) and U(V) standards, showed evidence for U(V) ingress into samples as the Fe(II) mediated reaction progressed, reaching approximately 26% U(V) after 10 days. Linear combination fits (LCF) of L_{III} edge XANES were also performed for Fe(II) reacted samples, using the synthesized U(VI) goethite and U(V) goethite as standards. For samples taken at 6 h, 1 day, and 10 days LCF of L_{III} edge XANES (13%, 14%, and 28% U(V), respectively, Table S2) correlate very well with the ITFA M_{IV} edge data (11%, 14%, and 26% U(V), respectively, Table S1). This provides further confidence in the accuracy of the L_{III} edge XANES data reported here, which showed that by 30 days approximately 52% reduction to U(V) had occurred (Figure 2B). Furthermore, L_{III} edge XANES data showed approximately 45% U(V) in the 53 weeks sample, indicating that the reaction end point had been reached by 30 days. As the experimental system had a significant molar excess of approximately 60 Fe(II):U(VI), there was no observable decrease in aqueous Fe(II) indicative of electron transfer to U(VI). However, XANES data clearly indicates that a significant fraction of incorporated U(VI) (approximately 50%) has been reduced to U(V) during reaction with Fe(II).

The extent of electron transfer within iron (oxyhydr)oxide phases is largely dependent on surface defects, with simulations suggesting that electrons may penetrate up to 2 nm into the goethite structure for a smooth defect free surface, and up to 8 nm for a very rough surface.[27,29,38] Given the highly crystalline goethite produced here (Figure S1), electron transfer was likely concentrated in the outermost atomic layers of the crystal, which are enriched in U(VI). Therefore, the U(VI) reduction pathway is thought to be dominated by U(VI) bound in the near surface region of goethite. This proposed reduction mechanism would result in goethite particles consisting of an unchanged core of incorporated U(VI) and a near surface region where electron transfer has led to the formation of U(V). To investigate this hypothesis, near surface U was extracted from a 30 day Fe(II) reacted sample using 0.4 M HCl. Analysis of L_{III} edge XANES spectra on the resulting solid showed that the 0.4 M HCl washed 30 day sample was nearly identical to the 0.4 M HCl washed U(VI) goethite starting material (Figure S8, Table S2). This demonstrated that all the U(V) was removed during the acid extraction, confirming that U(V) was only present in a near surface environment and that the goethite particle core remained largely unchanged following electron transfer from Fe(II).

To further probe uranium speciation, U L_{III} edge extended X ray absorption fine structure (EXAFS) spectra were collected. The EXAFS fitting approach used was similar to that previously described,[10] with U−O and U−Fe shells simultaneously refined. Once a full model had been constructed, the statistical validity of each O and Fe shell was then confirmed using F tests (Table S3).[57] For the U(VI) goethite starting material, the best fit model included oxygen backscatterers split across shells at 1.82, 2.03, 2.23, and 2.42 Å (Table 1). Additionally, the fit included 7 different U−Fe interatomic distances, extending out to 5.90 Å. The U−Fe distances and coordination numbers observed in the best fit are consistent with the Fe−Fe shells in pure goethite, indicating that the U is directly replacing Fe in the structure. Here, the four nearest U−Fe distances are elongated by approximately 0.2 Å compared to the Fe−Fe distances in goethite, as expected for the incorporation of U(VI) into an Fe(III) site given the increased electrostatic repulsion and ionic radius of U(VI) compared to Fe(III). Furthermore, atomic simulations have predicted the elongation of U−Fe distances on incorporation of U into an occupied Fe goethite site, again consistent with the current best fit described here.[58]

The overall distribution of U−O bond lengths modeled for the U(VI) goethite starting material is indicative of U(VI) in a mixture of 6 and 7 fold coordination environments. Specifically, previous studies have shown that U(VI) in octahedral coordination (6 fold) have maximum U−O equatorial distances of 2.34 Å.[59] Therefore, the presence of U−O distances at 2.42 Å suggests a higher coordination

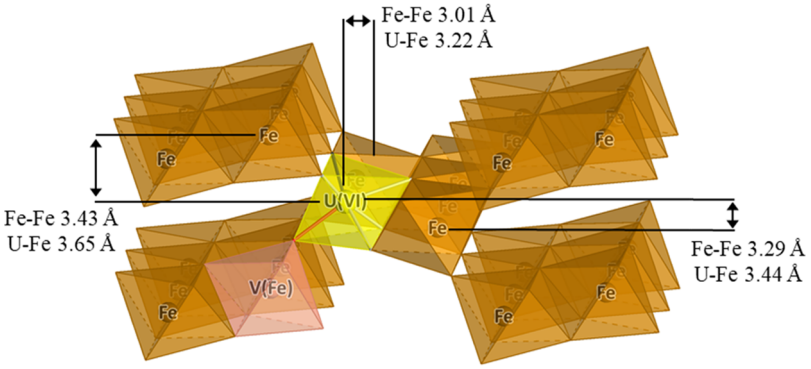

Figure 3. Structure of U(VI) incorporated goethite derived from the best fit EXAFS model (Table 1). V(Fe) = corner sharing vacancy; red line indicates shorter U−O bond.

number. In addition, the average U−O equatorial bond length for the U(VI) goethite described here is 2.33 Å, which lies between the determined averages for U(VI) in 6 fold (2.28(5) Å) and 7 fold (2.37(9) Å) coordination from a range of compounds.[59] Interestingly, for the U(VI) goethite in this study, the fit included a coordination number of 0.8 for a short U(VI) O bond at 1.82 Å. This short U−O distance is typically indicative of uranyl species (e.g., surface adsorbed uranyl species), but all samples were treated with a 4 mM acid leach (<pH 2.5), therefore it is unlikely that any adsorbed uranyl species were retained in this experiment. To investigate whether this feature was due to a mixed U coordination (i.e., presence of near surface bound U(VI) uranyl species), an additional EXAFS analysis was conducted on a sample from which all near surface U had been extracted with 0.4 M HCl (Table S3). EXAFS analysis confirmed that the short U−O distance (1.82 Å) was retained after removal of near surface U, with oxygen backscatterers at 1.82, 1.99, 2.18, and 2.35 Å. Therefore, the only change to the U coordination environment was a slight shortening in atomic distances (≤0.07 Å), leading to an average U−O equatorial distance of 2.25 Å, indicative of a predominantly 6 fold U(VI) coordination (2.28(5) Å; Burns et al.).[59] Moreover, U(VI) incorporated within the bulk of the goethite particles contains shorter U−O equatorial oxygens, up to a maximum of 2.35(2) Å.[59] Therefore, the fit described here, on removal of near surface U (Table S3), is consistent with U(VI) incorporated within the bulk/core of the particles being predominantly 6 fold coordinated. However, the elongated U−O equatorial distances described prior to acid extraction (i.e., 2.42 Å) are more typical of 7 fold coordination.[59] Therefore, we suggest that the U(VI) in the near surface of the goethite particles are likely to be present within a distorted 7 fold coordination environment.

For comparison, a U(V) goethite was also synthesized and analyzed by U L_{III} edge EXAFS.[16] Here, the best fit model produced 5.2 oxygen backscatterers at 2.17 Å and 1.8 oxygen backscatterers at 2.45 Å. Again, 7 different interatomic U−Fe distances were also identified and confirmed using F tests (Table S3), strongly suggesting an incorporated U(V) species directly replacing Fe(III) in goethite. In contrast to U(VI) goethite, the U(V) ion showed no evidence for a short 1.82 Å oxygen backscatterer, and the fit was consistent with a uranate like coordination environment. Interestingly, the U−Fe coordination environments in both U(V) and U(VI) samples were consistent, showing that the local environment of the U in both oxidation states is remarkably similar beyond the first coordination shell. However, previous atomic simulations for U(V) incorporated goethite produced an average U−O distance of 2.11 Å for 6 fold coordination, compared to 2.20 Å for 7 fold coordination.[58] Given that the U(V) goethite fit described here has an average U−O of 2.24 Å, this suggests an incorporated 7 fold coordination environment, similar to the U(V) site found in the wyartite ($CaU(V)(U(VI)O_2)_2(CO_3)O_4(OH)\cdot 7H_2O$) structure (i.e., 4 × 2.06−2.14 and 3 × 2.44−2.48 Å).[60]

For U(V), a room temperature synthesis of a pure U(V) goethite phase was possible (0.3 mM Fe(II), pH 7.5, 11 days reaction). By contrast, a hydrothermal synthesis (180 °C, pH 14, 24 h) was required to produce U(VI) goethite. The concentration of U incorporated into U(V) goethite was higher than that of U(VI) goethite, at 0.83 wt % vs 0.21 wt % for U(V) and U(VI), respectively. This may indicate that the U(V) uranate like incorporation environment is more favorable for incorporation relative to the distorted octahedral moiety found in U(VI) goethite. These results seem to be supported by past work which has focused on the use of reducing conditions to incorporate U, which produces predominantly U(V) incorporated goethite, with U(VI) incorporation thought to be unlikely due to the destabilizing effect of the uranyl moiety.[6,12−16] Interestingly, although corner sharing Fe vacancies enable U(VI) uranyl stabilization in hematite, the formation of equivalent vacancies is expected to have a destabilizing effect in goethite, due to disruption of the edge sharing arrangement of the goethite mineral structure.[26,51] Consequently, the presence of U(VI) is thought to be more stable in hematite, thereby favoring hematite formation,[9] and in the current study increased concentrations of initial U(VI) (635 ppm vs 200 ppm) did in fact produce mixed goethite/hematite phases (Figure S2, SI). Therefore, prior studies have suggested that the incorporation of U into goethite is facilitated by the use of reducing conditions which favor the sequestration of U(V) as a more uranate like moiety.[16,26] The weaker axial bonds in U(V) enable the formation of a more symmetrical uranate coordination, thereby reducing distortion of the overall goethite structure.[16,26]

Further inspection of the best fit for the U(VI) incorporated goethite EXAFS data showed a slight decrease in the Fe coordination number at the corner sharing U−Fe_3 (n = 3) in comparison to unsubstituted goethite (n = 4) (Table 1). This may suggest that the formation of a U−O bond at 1.82 Å could be associated with the presence of an Fe(III) vacancy in the U(VI) goethite structure, located adjacent to this shorter U−O bond (Figure 3). As stated previously, the incorporation of a uranyl moiety (with two axial bonds) has been assumed to be

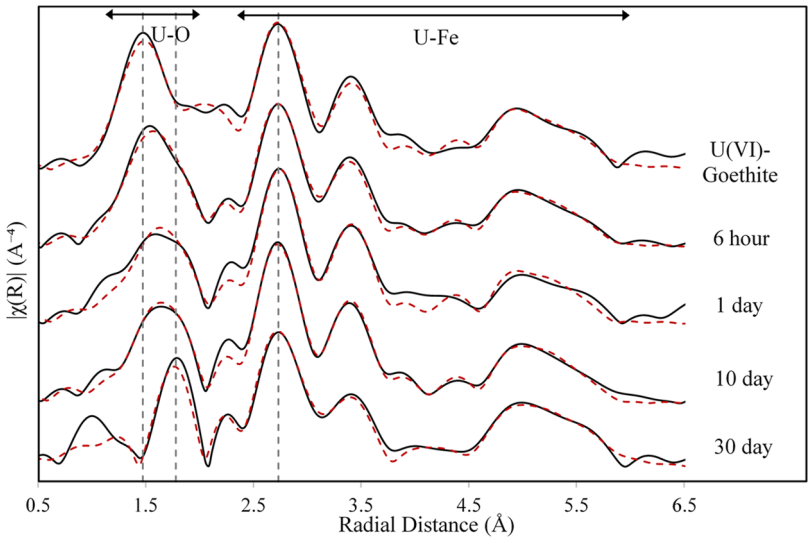

Figure 4. Fourier transform data of the L_{III} edge EXAFS for samples of U(VI) goethite reacted with aqueous Fe(II) over various time points. EXAFS data are included in SI, Figure S10. Solid black lines and dotted red lines represent the real data and the associated fits respectively, with key U−O and U−Fe peak positions indicated by vertical dotted gray lines.

highly destabilizing to the goethite structure if two *trans* Fe vacancies (as found in hematite) were required to accom modate this moiety.[26,61] Given that there would be less structural destabilization for just one Fe vacancy, this could provide insight into the presence of a single, shorter U−O bond for the incorporated U(VI) in the current work. Indeed, a fit produced for U(VI) incorporated goethite using ab initio molecular dynamics (AIMD) modeling and a single Fe edge sharing vacancy did contain a single short U−O bond at 1.89 Å,[62] similar to our experimental fits for the hydrothermally synthesized U(VI) incorporated goethite. Therefore, a single Fe vacancy is a possible explanation for the distorted uranyl like configuration presented here, and provides a mechanism for charge compensation related to the substitution of U(VI) for Fe(III) in the goethite structure.

Analysis of the EXAFS fits for the Fe(II) reacted samples reveal that there are subtle changes in the U−O coordination environment over time, which can be seen as a gradual shift in the U−O peak position in the Fourier transform (Figure 4). The EXAFS fit for the U(VI) goethite starting material included two short oxygen bonds, with 0.8 oxygen back scatterers at 1.82 Å and 0.8 oxygens at 2.03 Å. However, after 30 days reaction, the two short U−O backscatterers at 1.82 and 2.03 Å were replaced by 1 oxygen backscatterer at 1.98 Å (Table 1; Figure 4). The linear combination fits (LCF) of the L_{III} edge XANES show that 52% of the U(VI) is reduced to U(V) after 30 days reaction with aqueous Fe(II), therefore the 30 days EXAFS fit is likely the average of two distinct U(V) and U(VI) coordination environments. By 30 days approx imately 50% uranium is retained in the distorted incorporated U(VI) octahedral coordination, as evidenced by the decrease from approximately 2 oxygen backscatters at 1.82 and 2.03 Å (U(VI) goethite starting material), to 1 oxygen backscatterer at an approximate median distance of 1.98 Å. An increase in coordination number (2.2 to 3) for a uranate like oxygen distance at 2.23 Å is consistent with the second uranium environment being a uranate U(V) coordination. Moreover, the U−Fe coordination environment was consistent across all samples (Table 1). These observations provide further confidence that U remained incorporated within the goethite structure, even with the extensive changes in coordination environment associated with approximately 50% of the distorted U(VI) moiety undergoing reduction to a uranate like U(V) during reaction with aqueous Fe(II).

XAS analysis has confirmed that the U(VI) reduction pathway is dominated by U(VI) bound in the near surface region of goethite, with up to 52% U(VI) reduced to U(V) on reaction with Fe(II). During this reaction, the outermost layers (2%) of U(VI) goethite underwent Fe atom exchange, with approximately 40% of the U located within this 2% near surface region (Figure S3, SI). Therefore, there is the possibility of both direct and indirect electron transfer interactions between Fe(II) and U(VI), as near surface U(VI) may be exposed to the Fe(II) bearing solution phase during recrystallization of the outermost 2% goethite layers. Consequently, in addition to electron transfer from nearby adsorbed Fe(II), aqueous Fe(II) may also directly bind to exposed U(VI), with subsequent reduction to U(V). As suggested by Massey et al.,[16] the weakening of axial bonds on reduction to U(V) apparently enables a shift to a U(V) uranate like coordination, which creates less distortion to the goethite structure and so appears to form preferentially to a U(V) uranyl moiety.[16,26] Electron transfer from Fe(II) to incorporated U(VI) then continues, until near surface U(VI) has been reduced and retained as a uranate like U(V) in the outermost layers of the goethite structure.

Environmental Implications. Using a combination of U L_{III} edge XAS and M_{IV} edge HERFD XANES, the structure and stability of a novel U(VI) incorporated goethite has been explored. A mechanism has also been proposed for the behavior of U during the reaction of U(VI) goethite with aqueous Fe(II). Near surface U(VI) was found to undergo reduction on exposure to Fe(II), forming incorporated U(V) with a uranate like coordination. Electron transfer only occurred within the outermost layers of goethite and the U(VI) speciation in the inner particle core was largely preserved, with minimal recrystallization (2%) observed following electron transfer. These results suggest that U may be retained within the goethite structure during the develop ment of iron reducing conditions in the environment, with no

evidence for U release reported here during reaction with Fe(II). Therefore, unless a dissolution process or phase transformation occurs, U may be retained in the solid phase in the long term. This further develops the evolving concept of an iron (oxyhydr)oxide barrier to radionuclide migration, suggesting that long term immobilization of U species may occur in contaminated land and GDF scenarios.

ASSOCIATED CONTENT

Supporting Information

The Supporting Information is available free of charge at https://pubs.acs.org/doi/10.1021/acs.est.1c06197.

Additional information on the X ray diffraction (XRD), acid digestion, ^{57}Fe tracer experiment, M_{IV} edge XANES, and L_{III} edge EXAFS (PDF)

AUTHOR INFORMATION

Corresponding Author

Samuel Shaw − *Research Centre for Radwaste Disposal and Williamson Research Centre for Molecular Environmental Science, Department of Earth and Environmental Sciences, The University of Manchester, Manchester M13 9PL, United Kingdom;* orcid.org/0000 0002 6353 5454; Email: sam.shaw@manchester.ac.uk

Authors

Olwen Stagg − *Research Centre for Radwaste Disposal and Williamson Research Centre for Molecular Environmental Science, Department of Earth and Environmental Sciences, The University of Manchester, Manchester M13 9PL, United Kingdom;* orcid.org/0000 0002 3365 4110

Katherine Morris − *Research Centre for Radwaste Disposal and Williamson Research Centre for Molecular Environmental Science, Department of Earth and Environmental Sciences, The University of Manchester, Manchester M13 9PL, United Kingdom;* orcid.org/0000 0002 0716 7589

Andy Lam − *Peter A. Rock Thermochemistry Laboratory and NEAT ORU, University of California Davis, Davis, California 95616, United States;* orcid.org/0000 0002 5940 4021

Alexandra Navrotsky − *School of Molecular Sciences and Navrotsky Eyring Center for Materials of the Universe, Arizona State University, Tempe, Arizona 85287, United States;* orcid.org/0000 0002 3260 0364

Jesús M. Velázquez − *Department of Chemistry, University of California—Davis, Davis, California 95616, United States;* orcid.org/0000 0003 2790 0976

Bianca Schacherl − *Institute for Nuclear Waste Disposal (INE), Karlsruhe Institute of Technology, Karlsruhe 76131, Germany;* orcid.org/0000 0003 4542 0108

Tonya Vitova − *Institute for Nuclear Waste Disposal (INE), Karlsruhe Institute of Technology, Karlsruhe 76131, Germany;* orcid.org/0000 0002 3117 7701

Jörg Rothe − *Institute for Nuclear Waste Disposal (INE), Karlsruhe Institute of Technology, Karlsruhe 76131, Germany;* orcid.org/0000 0001 5366 2129

Jurij Galanzew − *Institute for Nuclear Waste Disposal (INE), Karlsruhe Institute of Technology, Karlsruhe 76131, Germany*

Anke Neumann − *School of Engineering, Newcastle University, Newcastle upon Tyne NE1 7RU, United Kingdom*

Paul Lythgoe − *Manchester Analytical Geochemistry Unit, The University of Manchester, Manchester M13 9PL, United Kingdom*

Liam Abrahamsen Mills − *National Nuclear Laboratory, Warrington, Cheshire WA3 6AE, United Kingdom*

Author Contributions

The manuscript was written through contributions of all authors. All authors have given approval to the final version of the manuscript.

Funding

EPSRC and National Nuclear Laboratory cofunded the PhD studentship to O.S. via the Next Generation Nuclear CDT (EP/L0/5390/1).

Notes

The authors declare no competing financial interest.

ACKNOWLEDGMENTS

Diamond Light Source provided a beamtime award (SP21441), and we thank Fred Mosselmanns and Shusaku Hayama for their beamline assistance. We also acknowledge access to the EPSRC NNUF RADER Facility (EP/T011300/1) for analyses performed in this work. We thank Ilya Strashnov for help with data acquisition, and Alana Mcnulty and Hannah Roberts for providing a U(VI) and U(V) M_{IV} edge standard, respectively. We thank the Institute for Beam Physics and Technology (IBPT) for the operation of the storage ring, the Karlsruhe Research Accelerator (KARA). We thank Luke T. Townsend for helpful comments during manuscript review. J.M.V. acknowledges funding by the Nuclear Regulatory Commission (31310019M0009) through the Advancing Scientific Careers to Enhance Nuclear Technologies (ASCENT) program.

REFERENCES

(1) Newsome, L.; Morris, K.; Lloyd, J. R. The Biogeochemistry and Bioremediation of Uranium and Other Priority Radionuclides. *Chem. Geol.* **2014**, *363*, 164−184.

(2) Morris, K.; Law, G. T. W.; Bryan, N. D. Geodisposal of Higher Activity Wastes. In *Nuclear Power and the Environment*; Hester, R. E., Harrison, R. M., Eds.; Royal Society of Chemistry: London, 2011; pp 129−151.

(3) Ma, B.; Charlet, L.; Fernandez Martinez, A.; Kang, M.; Madé, B. A Review of the Retention Mechanisms of Redox Sensitive Radio nuclides in Multi Barrier Systems. *Appl. Geochem.* **2019**, *100*, 414−431.

(4) Marshall, T. A.; Morris, K.; Law, G. T. W.; Mosselmans, J. F. W.; Bots, P.; Roberts, H.; Shaw, S. Uranium Fate during Crystallization of Magnetite from Ferrihydrite in Conditions Relevant to the Disposal of Radioactive Waste. *Mineral. Mag.* **2015**, *79* (6), 1265−1274.

(5) Massey, M. S.; Lezama Pacheco, J. S.; Michel, F. M.; Fendorf, S. Uranium Incorporation into Aluminum Substituted Ferrihydrite during Iron(II) Induced Transformation. *Environ. Sci. Process. Impacts* **2014**, *16* (9), 2137−2144.

(6) Boland, D. D.; Collins, R. N.; Payne, T. E.; Waite, T. D. Effect of Amorphous Fe(III) Oxide Transformation on the Fe(II) Mediated Reduction of U(VI). *Environ. Sci. Technol.* **2011**, *45* (4), 1327−1333.

(7) Roberts, H. E.; Morris, K.; Law, G. T. W.; Mosselmans, J. F. W.; Bots, P.; Kvashnina, K.; Shaw, S. Uranium(V) Incorporation Mechanisms and Stability in Fe(II)/Fe(III) (Oxyhydr)Oxides. *Environ. Sci. Technol. Lett.* **2017**, *4* (10), 421−426.

(8) Pidchenko, I.; Kvashnina, K. O.; Yokosawa, T.; Finck, N.; Bahl, S.; Schild, D.; Polly, R.; Bohnert, E.; Rossberg, A.; Göttlicher, J.; Dardenne, K.; Rothe, J.; Schäfer, T.; Geckeis, H.; Vitova, T. Uranium Redox Transformations after U(VI) Coprecipitation with Magnetite Nanoparticles. *Environ. Sci. Technol.* **2017**, *51* (4), 2217−2225.
(9) Duff, M. C.; Coughlin, J. U.; Hunter, D. B. Uranium Co Precipitation with Iron Oxide Minerals. *Geochim. Cosmochim. Acta* **2002**, *66* (20), 3533−3547.
(10) Marshall, T. A.; Morris, K.; Law, G. T. W.; Livens, F. R.; Mosselmans, J. F. W.; Bots, P.; Shaw, S. Incorporation of Uranium into Hematite during Crystallization from Ferrihydrite. *Environ. Sci. Technol.* **2014**, *48* (7), 3724−3731.
(11) Ilton, E. S.; Pacheco, J. S. L.; Bargar, J. R.; Shi, Z.; Liu, J.; Kovarik, L.; Engelhard, M. H.; Felmy, A. R. Reduction of U(VI) Incorporated in the Structure of Hematite. *Environ. Sci. Technol.* **2012**, *46* (17), 9428−9436.
(12) Nico, P. S.; Stewart, B. D.; Fendorf, S. Incorporation of Oxidized Uranium into Fe (Hydr)Oxides during Fe(II) Catalyzed Remineralization. *Environ. Sci. Technol.* **2009**, *43* (19), 7391−7396.
(13) Doornbusch, B.; Bunney, K.; Gan, B. K.; Jones, F.; Gräfe, M. Iron Oxide Formation from $FeCl_2$ Solutions in the Presence of Uranyl (UO_2^{2+}) Cations and Carbonate Rich Media. *Geochim. Cosmochim. Acta* **2015**, *158*, 22−47.
(14) Boland, D. D.; Collins, R. N.; Glover, C. J.; Payne, T. E.; Waite, T. D. Reduction of U(VI) by Fe(II) during the Fe(II) Accelerated Transformation of Ferrihydrite. *Environ. Sci. Technol.* **2014**, *48* (16), 9086−9093.
(15) Stewart, B. D.; Nico, P. S.; Fendorf, S. Stability of Uranium Incorporated into Fe (Hydr)Oxides under Fluctuating Redox Conditions. *Environ. Sci. Technol.* **2009**, *43* (13), 4922−4927.
(16) Massey, M. S.; Lezama Pacheco, J. S.; Jones, M. E.; Ilton, E. S.; Cerrato, J. M.; Bargar, J. R.; Fendorf, S. Competing Retention Pathways of Uranium upon Reaction with Fe(II). *Geochim. Cosmochim. Acta* **2014**, *142*, 166−185.
(17) Cumberland, S. A.; Douglas, G.; Grice, K.; Moreau, J. W. Uranium Mobility in Organic Matter Rich Sediments: A Review of Geological and Geochemical Processes. *Earth Sci. Rev.* **2016**, *159*, 160−185.
(18) Townsend, L. T.; Morris, K.; Lloyd, J. R. Microbial Transformations of Radionuclides in Geodisposal Systems. In *The Microbiology of Nuclear Waste Disposal*; Elsevier: Amsterdam, 2021; pp 245−265.
(19) Ekstrom, A. Kinetics and Mechanism of the Disproportionation of Uranium(V). *Inorg. Chem.* **1974**, *13* (9), 2237−2241.
(20) Waite, T. D.; Davis, J. A.; Payne, T. E.; Waychunas, G. A.; Xu, N. Uranium(VI) Adsorption to Ferrihydrite: Application of a Surface Complexation Model. *Geochim. Cosmochim. Acta* **1994**, *58* (24), 5465−5478.
(21) Sherman, D. M.; Peacock, C. L.; Hubbard, C. G. Surface Complexation of U(VI) on Goethite (α FeOOH). *Geochim. Cosmochim. Acta* **2008**, *72* (2), 298−310.
(22) Li, D.; Kaplan, D. I. Sorption Coefficients and Molecular Mechanisms of Pu, U, Np, Am and Tc to Fe (Hydr)Oxides: A Review. *J. Hazard. Mater.* **2012**, *243*, 1−18.
(23) Boglaienko, D.; Levitskaia, T. G. The Abiotic Reductive Removal and Subsequent Incorporation of Tc(IV) into Iron Oxides: A Frontier Review. *Environ. Sci.: Nano* **2019**, *6* (12), 3492−3500.
(24) Cornell, R. M.; Schwertmann, U. Synthesis. In *The Iron Oxides: Structure, Properties, Reactions, Occurences and Uses*; Wiley VCH Verlag GmbH & Co. KGaA: Weinheim, 2003; pp 525−540.
(25) Guo, H.; Barnard, A. S. Naturally Occurring Iron Oxide Nanoparticles: Morphology, Surface Chemistry and Environmental Stability. *J. Mater. Chem. A* **2013**, *1*, 27−42.
(26) Soltis, J. A.; McBriarty, M. E.; Qafoku, O.; Kerisit, S. N.; Nakouzi, E.; De Yoreo, J. J.; Ilton, E. S. Can Mineral Growth by Oriented Attachment Lead to Incorporation of Uranium(VI) into the Structure of Goethite? *Environ. Sci.: Nano* **2019**, *6* (10), 3000−3009.
(27) Notini, L.; Latta, D. E.; Neumann, A.; Pearce, C. I.; Sassi, M.; N'Diaye, A. T.; Rosso, K. M.; Scherer, M. M. The Role of Defects in Fe(II) Goethite Electron Transfer. *Environ. Sci. Technol.* **2018**, *52* (5), 2751−2759.
(28) Williams, A. G. B.; Scherer, M. M. Spectroscopic Evidence for Fe(II) Fe(III) Electron Transfer at the Iron Oxide Water Interface. *Environ. Sci. Technol.* **2004**, *38* (18), 4782−4790.
(29) Zarzycki, P.; Rosso, K. M. Energetics and the Role of Defects in Fe(II) Catalyzed Goethite Recrystallization from Molecular Simu lations. *ACS Earth Sp. Chem.* **2019**, *3* (2), 262−272.
(30) Notini, L.; Latta, D. E.; Neumann, A.; Pearce, C. I.; Sassi, M.; N'diaye, A. T.; Rosso, K. M.; Scherer, M. M. A Closer Look at Fe(II) Passivation of Goethite. *ACS Earth Sp. Chem.* **2019**, *3* (12), 2717−2725.
(31) Yanina, S. V.; Rosso, K. M. Linked Reactivity at Mineral Water Interfaces through Bulk Crystal Conduction. *Science* **2008**, *320* (5873), 218−222.
(32) Frierdich, A. J.; Helgeson, M.; Liu, C.; Wang, C.; Rosso, K. M.; Scherer, M. M. Iron Atom Exchange between Hematite and Aqueous Fe(II). *Environ. Sci. Technol.* **2015**, *49* (14), 8479−8486.
(33) Gorski, C. A.; Handler, R. M.; Beard, B. L.; Pasakarnis, T.; Johnson, C. M.; Scherer, M. M. Fe Atom Exchange between Aqueous Fe^{2+} and Magnetite. *Environ. Sci. Technol.* **2012**, *46* (22), 12399−12407.
(34) Handler, R. M.; Beard, B. L.; Johnson, C. M.; Scherer, M. M. Atom Exchange between Aqueous Fe(II) and Goethite: An Fe Isotope Tracer Study. *Environ. Sci. Technol.* **2009**, *43* (4), 1102−1107.
(35) Handler, R. M.; Frierdich, A. J.; Johnson, C. M.; Rosso, K. M.; Beard, B. L.; Wang, C.; Latta, D. E.; Neumann, A.; Pasakarnis, T.; Premaratne, W. A. P. J.; Scherer, M. M. Fe(II) Catalyzed Recrystallization of Goethite Revisited. *Environ. Sci. Technol.* **2014**, *48* (19), 11302−11311.
(36) Hua, J.; Chen, M.; Liu, C.; Li, F.; Long, J.; Gao, T.; Wu, F.; Lei, J.; Gu, M. Cr Release from Cr Substituted Goethite during Aqueous Fe(II) Induced Recrystallization. *Minerals* **2018**, *8* (9), 367.
(37) Burton, E. D.; Hockmann, K.; Karimian, N. Antimony Sorption to Goethite: Effects of Fe(II) Catalyzed Recrystallization. *ACS Earth Sp. Chem.* **2020**, *4* (3), 476−487.
(38) Southall, S. C.; Micklethwaite, S.; Wilson, S. A.; Frierdich, A. J. Changes in Crystallinity and Tracer Isotope Distribution of Goethite during Fe(II) Accelerated Recrystallization. *ACS Earth Sp. Chem.* **2018**, *2* (12), 1271−1282.
(39) Frierdich, A. J.; Catalano, J. G. Fe(II) Mediated Reduction and Repartitioning of Structurally Incorporated Cu, Co, and Mn in Iron Oxides. *Environ. Sci. Technol.* **2012**, *46* (20), 11070−11077.
(40) Frierdich, A. J.; Scherer, M. M.; Bachman, J. E.; Engelhard, M. H.; Rapponotti, B. W.; Catalano, J. G. Inhibition of Trace Element Release during Fe(II) Activated Recrystallization of Al , Cr , and Sn Substituted Goethite and Hematite. *Environ. Sci. Technol.* **2012**, *46* (18), 10031−10039.
(41) Frierdich, A. J.; Catalano, J. G. Controls on Fe(II) Activated Trace Element Release from Goethite and Hematite. *Environ. Sci. Technol.* **2012**, *46* (3), 1519−1526.
(42) Schwertmann, U.; Cornell, R. M. Goethite. In *Iron Oxides in the Laboratary*; Schwertmann, U., Cornell, R. M., Eds.; Wiley VCH Verlag GmbH: Weinheim, 2000; pp 67−92.
(43) Guo, Z.; Li, Y.; Wu, W. Sorption of U(VI) on Goethite: Effects of PH, Ionic Strength, Phosphate, Carbonate and Fulvic Acid. *Appl. Radiat. Isot.* **2009**, *67* (6), 996−1000.
(44) Dodge, C. J.; Francis, A. J.; Gillow, J. B.; Halada, G. P.; Eng, C.; Clayton, C. R. Association of Uranium with Iron Oxides Typically Formed on Corroding Steel Surfaces. *Environ. Sci. Technol.* **2002**, *36* (16), 3504−3511.
(45) Joshi, P.; Gorski, C. A. Anisotropic Morphological Changes in Goethite during Fe^{2+} Catalyzed Recrystallization. *Environ. Sci. Technol.* **2016**, *50* (14), 7315−7324.
(46) Viollier, E.; Inglett, P. W.; Hunter, K.; Roychoudhury, A. N.; Van Cappellen, P. The Ferrozine Method Revisited: Fe(II)/Fe(III) Determination in Natural Waters. *Appl. Geochem.* **2000**, *15* (6), 785−790.

(47) Cornell, R. M.; Schwertmann, U. Solubility. In *The Iron Oxides: Structure, Properties, Reactions, Occurences and Uses*; Wiley VCH Verlag GmbH & Co. KGaA: Weinheim, 2003; pp 201−220.
(48) Vitova, T.; Pidchenko, I.; Schild, D.; Prüßmann, T.; Montoya, V.; Fellhauer, D.; Gaona, X.; Bohnert, E.; Rothe, J.; Baker, R. J.; Geckeis, H. Competitive Reaction of Neptunium(V) and Uranium (VI) in Potassium Sodium Carbonate Rich Aqueous Media: Speci ation Study with a Focus on High Resolution X Ray Spectroscopy. *Inorg. Chem.* **2020**, *59* (1), 8−22.
(49) Vitova, T.; Pidchenko, I.; Fellhauer, D.; Bagus, P. S.; Joly, Y.; Pruessmann, T.; Bahl, S.; Gonzalez Robles, E.; Rothe, J.; Altmaier, M.; Denecke, M. A.; Geckeis, H. The Role of the 5f Valence Orbitals of Early Actinides in Chemical Bonding. *Nat. Commun.* **2017**, *8* (1), 1−9.
(50) Neumann, A.; Wu, L.; Li, W.; Beard, B. L.; Johnson, C. M.; Rosso, K. M.; Frierdich, A. J.; Scherer, M. M. Atom Exchange between Aqueous Fe(II) and Structural Fe in Clay Minerals. *Environ. Sci. Technol.* **2015**, *49* (5), 2786−2795.
(51) Frierdich, A. J.; McBride, A.; Tomkinson, S.; Southall, S. C. Nickel Cycling and Negative Feedback on Fe(II) Catalyzed Recrystallization of Goethite. *ACS Earth Sp. Chem.* **2019**, *3* (9), 1932−1941.
(52) Latta, D. E.; Bachman, J. E.; Scherer, M. M. Fe Electron Transfer and Atom Exchange in Goethite: Influence of Al Substitution and Anion Sorption. *Environ. Sci. Technol.* **2012**, *46* (19), 10614−10623.
(53) Vettese, G. F.; Morris, K.; Natrajan, L. S.; Shaw, S.; Vitova, T.; Galanzew, J.; Jones, D. L.; Lloyd, J. R. Multiple Lines of Evidence Identify U(V) as a Key Intermediate during U(VI) Reduction by Shewanella Oneidensis MR1. *Environ. Sci. Technol.* **2020**, *54* (4), 2268−2276.
(54) Rothe, J.; Altmaier, M.; Dagan, R.; Dardenne, K.; Fellhauer, D.; Gaona, X.; Corrales, E. G. R.; Herm, M.; Kvashnina, K. O.; Metz, V.; Pidchenko, I.; Schild, D.; Vitova, T.; Geckeis, H. Fifteen Years of Radionuclide Research at the KIT Synchrotron Source in the Context of the Nuclear Waste Disposal Safety Case. *Geosciences* **2019**, *9* (2), 91.
(55) Pidchenko, I.; Heberling, F.; Kvashnina, K. O. K.; Finck, N.; Schild, D.; Bohnert, E.; Schäfer, T.; Rothe, J.; Geckeis, H.; Vitova, T. Aqueous U(VI) Interaction with Magnetite Nanoparticles in a Mixed Flow Reactor System: HR XANES Study. *J. Phys.: Conf. Ser.* **2016**, *712*, 012086.
(56) Roßberg, A.; Reich, T.; Bernhard, G. Complexation of Uranium(VI) with Protocatechuic Acid Application of Iterative Transformation Factor Analysis to EXAFS Spectroscopy. *Anal. Bioanal. Chem.* **2003**, *376* (5), 631−638.
(57) Downward, L.; Booth, C. H.; Lukens, W. W.; Bridges, F. A Variation of the F Test for Determining Statistical Relevance of Particular Parameters in EXAFS Fits. *AIP Conf. Proc.* **2006**, *882*, 129−131.
(58) Kerisit, S.; Felmy, A. R.; Ilton, E. S. Atomistic Simulations of Uranium Incorporation into Iron (Hydr)Oxides. *Environ. Sci. Technol.* **2011**, *45* (7), 2770−2776.
(59) Burns, P. C.; Ewing, R. C.; Hawthorne, F. C. The Crystal Chemistry of Hexavalent Uranium; Polyhedron Geometries, Bond Valence Parameters, and Polymerization of Polyhedra. *Can. Mineral.* **1997**, *35* (6), 1551−1570.
(60) Burns, P. C.; Finch, R. J. Wyartite: Crystallographic Evidence for the First Pentavalent Uranium Mineral. *Am. Mineral.* **1999**, *84* (9), 1456−1460.
(61) McBriarty, M. E.; Kerisit, S.; Bylaska, E. J.; Shaw, S.; Morris, K.; Ilton, E. S. Iron Vacancies Accommodate Uranyl Incorporation into Hematite. *Environ. Sci. Technol.* **2018**, *52* (11), 6282−6290.
(62) Kerisit, S.; Bylaska, E. J.; Massey, M. S.; McBriarty, M. E.; Ilton, E. S. Ab Initio Molecular Dynamics of Uranium Incorporated in Goethite (α FeOOH): Interpretation of X Ray Absorption Spectros copy of Trace Polyvalent Metals. *Inorg. Chem.* **2016**, *55* (22), 11736−11746.